Electro-active control of the viscous flow and tribological performance of ecolubricants based on phyllosilicate clay minerals and castor oil

Moisés García-Morales[a]*, Samuel D. Fernández-Silva[a], Claudia Roman[a], Miguel A. Delgado[a]

[a] *Departamento de Ingeniería Química, Centro de Investigación en Tecnología de Productos y Procesos Químicos (Pro2TecS), Campus de "El Carmen", Universidad de Huelva, 21071, Huelva (SPAIN)*

Corresponding author:

***Moisés García-Morales, PhD:** moises.garcia@diq.uhu.es
ORCID: 0000-0003-4153-487X

Other authors:

Samuel D. Fernández-Silva, MEng: samuel.fernandez@diq.uhu.es
ORCID: 0000-0001-6253-1497

Claudia Roman, PhD: claudia.roman@diq.uhu.es
ORCID: 0000-0002-7960-5832

Miguel A. Delgado, PhD: miguel.delgado@diq.uhu.es
ORCID: 0000-0003-0573-7987

ABSTRACT

Lubricating fluids with highly improved tribological performance very often entail the use of environmentally disrespectful formulations. Based on nanoclay dispersions in castor oil, the present research explores the development of simple and sustainable lubricants that enable an "active control" of the tribological behavior under the action of electric fields. Storage stable formulations with high electro-rheological (ER) performance were obtained with 2 wt.% organo-modified montmorillonites (OMMT) dispersions in castor oil. Their strong ER potential was assessed throught the dynamic yield stress values obtained from steady flow curves at 25 ºC under electric fields up to 4 kV/mm. Broadband dielectric spectroscopy measurements demonstrated a local maximum (or shoulder) in the dielectric loss, ε'', in the frequency range 5-10 kHz which is related to interfacial polarization. It was found that the OMMT nanoclays had a much greater ER potential than other types of nanoclay (e.g. halloysite nanotubes) that did not exhibit any polarization relaxation in ε''. Moreover, in general, a fairly good correlation of the yield stress values with the drop in the permittivity, $\Delta\varepsilon' = \varepsilon_0' - \varepsilon_\infty'$, was found for the OMMT nanoclays. Preliminary electro-tribological tests were carried out using a ball-on-three plates setup, with an optimal formulation prototype consisting in 2 wt.% Cloisite 15A dispersion in castor oil. The results demonstrated a reduction of up to 9 % of the friction coefficient in the mixed lubrication regime. This outcome, based on organo-modified layered nanosilicates dispersions in castor oil, revealed the feasibility of producing a "new generation" of lubricants which, with no need for hazardous chemicals, may assist in the development of a novel concept of lubrication through electric potentials.

Keywords: smart fluids; lubrication; electro-rheology; electro-tribology; nanoclay; sustainability**.**

1. Introduction

The continuous development of better lubricating oils has enabled to prolong their useful life and to protect the machines they are used in. Over the latest years, there has been extensive research on the preparation of lubricating fluids with improved tribological performance which have been shown to reduce friction and wear, among other properties. However, these fluids have often entailed complex formulations and, more importantly, the use of hazardous chemicals. About 50 % waste lubricants worldwide is estimated to end up in the environment (Madanhire and Mbohwa, 2016). Thus, there exists a big concern on the development of advanced but also environmentally friendly lubrication fluids. In this line, the most promising innovation might be linked to simple and environmentally respectful formulations of fluids with electro-rheological (ER) properties. These "smart" fluids may enable an instant and tailored control of the tribological performance of the lubricant film (Barber et al., 2005).

"Smart" or "functional" fluids are structured fluids which may undergo a dramatic change in some of their properties under the action of external stimuli, most often electric or magnetic fields. In consequence, they are especially interesting in applications where they act as electro-mechanical interfaces (Seo et al., 2011; 2012). The first studies on the electro-rheological phenomenon were published by Winslow (1947). In general, most of electro-rheological fluids consist in dispersions of polarizable particles in a non-conducting carrier (Roman et al., 2018). The particles are susceptible to orientate under an electric potential, forming structures that align perpendicular to the flow direction. Thus, the fluid rheological behavior instantly switches from Newtonian or slightly pseudoplastic to "Bingham fluid", this latter characterized by a yield stress which accounts for its electro-rheological potential. According to Ikazaki et al. (1998), the so-called "interfacial" polarization

(interface between particle and dispersing medium), also referred to as “Maxwell-Wagner” polarization, is one of the key factors behind such an extraordinary phenomenon.

Up to date, very few studies have reported the use of electro-rheological fluids in the field of lubrication (Peng and Zhu, 2005). The first studies (Kollias and Dimarogonas, 1994; Nikolakopoulos and Papadopoulos, 1996; 1998) demonstrated that it was possible to control high speed journal bearings with an electro-rheological fluid. Kimura et al. (1994) observed a reduction in the friction coefficient, in the boundary regime, due to the electro-viscous effect of a liquid crystal used as lubricant, whilst Korenaga et al. (1999) reported an increase in the lubricant film thickness in the hydrodynamic regime. More recently, Barber et al. (2005) conducted a study aimed to reduce friction and wear with an electro-rheological fluid based on cornstarch and mineral oil. Even though all these studies admitted a great lack of knowledge, they somehow opened the door to “a new concept of lubrication”.

The electro-rheological fluids can be categorized into two groups: the main group is constituted by dispersions of polarizable particles in a carrier, typically an oil; liquid crystals is a second group. However, the liquid crystals with interest for tribological applications entail complex formulations including chemicals which are potentially harmful to the environment (Kimura et al., 1994; Korenaga et al., 1999). Regarding the first group, lubrication may involve extreme pressure and temperature which limit the particle selection. Hence, among the many polarizable nanoparticles available (Liu and Choi, 2012), nanoclays show a great potential for tribological applications, not only for adapting to the lubrication conditions but also for their wide range of shapes and sizes (Ramos-Tejada et al., 2018). Phyllosilicates (layered nanosilicates) is the main category and includes, among many others, montmorillonite, bentonite and halloysite nanoclays. Montmorillonites and bentonites are constituted by two tetrahedral sheets of silica

sandwiching a central octahedral sheet of alumina (platelets). Negative charges at the interlayer galleries are counterbalanced by positive ions (Na+ mainly) which bind the platelets together. In modified montmorillonite and bentonite nanoclays, the sodium ions are replaced with quaternary ammonium salt ions in order to improve their dispersibility in organophilic media. Halloysite nanoclay is a phyllosilicate that naturally occurs in the form of nanotubes (Polanský et al., 2017). Finally, sepiolites, showing fiber-like structures, are not really layered nanosilicates since their blocks are not sheets but ribbons forming an open channel similar to that of zeolites (Garcia-Lopez et al., 2010).

A state-of-the-art review has revealed the dire need to carry out systematic investigations in order to advance the frontier of knowledge within the field of electro-functional lubricating fluids. In that sense, and based on the line of the currently promoted circular economy strategies, the present research has opted for nanoclay particles (natural and completely harmless) in castor oil (vegetable oil with good lubricity and high viscosity), so as to yield 100 % environmentally respectful formulations. In general, the tribology of lubricating fluids containing different types of clay minerals has been the subject matter of a list of published works. Thus, attempts on the use of these materials in the development of "greener" lubricants can be found involving: montmorillonite clay (Chizhik et al., 2019; Gorbacheva et al., 2020; Peña-Paras et al., 2018, 2019); halloysite nanotubes (Peña-Paras et al., 2017); sepiolite nanofibers (Martin-Alfonso et al., 2020); attapulgite nanofibers (Wang et al., 2011; Yu et al., 2021), combined layered-phosphate and layered-silicate (Chen et al., 2011); SiO_2 nanoparticles (Taha-Tijerina et al., 2019), among others. However, to the best of our knowledge, there is no evidence of a previous approach of this type in the field of lubrication under electric potentials. Hence, we report preliminary results on the development of sustainable lubricating fluids for the active control of the lubrication process by application of electric fields. The effect of the electric potential on

129 the friction coefficient was quantified by using a setup consisting of a ball-on-three plates
130 electro-tribocell coupled to a strain-controlled rheometer. A reduction in the friction
131 coefficient of up to 9 % at 50 V was observed in the mixed lubrication regime at 25 ºC with
132 a 2 wt.% Cloisite 15A dispersion in castor oil.

133 2. Materials and methods

134 2.1. Materials

135 A wide spectrum of nanoclays, both natural and organically modified and with different
136 morphologies, was considered. Table 1 lists the whole set of 12 nanoclays studied,
137 including category, commercial name, interlayer distance (by XRD), supplier, cation
138 exchange capacity and whether or not the naturally present Na^+ has been replaced with an
139 alkyl organocation. Castor oil was purchased from Guinama (Spain). Physicochemical
140 properties of this vegetable oil can be found elsewhere (Quinchia et al., 2010).

141 As will be later discussed, those nanoclays that presented poor storage stability in castor
142 oil after 24 hours were discarded from further analysis.

143

144 **Table 1.** Some characteristics of the natural and organo-modified nanoclays studied.

M o n t m o r i l l o n i t e (layered)				
Type	**Commercial Name**	**Organic modifier (cat. exch. cap.)**	**Interlayer distance, d_{001}**	**Supplier**
Natural	Cloisite Na^+	None (140 meq/100 g clay)	11.7 Å	Southern Clay Products (USA)
Organo (OMMT)	Cloisite 15A	2Me2HT (125 meq/100 g clay)	31.5 Å	Southern Clay Products (USA)
	Cloisite 20A	2Me2HT (95 meq/100 g clay)	24.2 Å	Southern Clay Products (USA)
	Nanofil 15	2Me2HT (93 meq/100 g clay)	28 Å	Sud Chemie (Germany)
	Nanofil SE3010	2MeBzHT (125 meq/100 g clay)	36 Å	Sud Chemie (Germany)
	Cloisite 30B	MeT2(EtOH) (90 meq/100 g clay)	18.5 Å	Southern Clay Products (USA)

B e n t o n i t e (layered)				
Natural	VoncanPlus	None	13.2 Å	Sepiolsa (Spain)
	VolcanGel	None	Unavailable	Sepiolsa (Spain)
H a l l o y s i t e (nanotubes)				
Natural	Halloysite	None	Unavailable	Sigma Aldrich
S e p i o l i t e (fiber-like)				
Natural	Pansil	None	Unavailable	Tolsa (Spain)
	Pangel S9	None	Unavailable	Tolsa (Spain)
	Pangel B20	None	Unavailable	Tolsa (Spain)

Bz: benzyl
EtOH: hydroxy-ethyl
HT: hydrogenated tallow (~ 65 wt.% c_{18}; ~ 30 wt.% c_{16}; ~ 5 wt.% c_{14})
Me: methyl
T: tallow (~ 65 wt.% c_{18}; ~ 30 wt.% c_{16}; ~ 5 wt.% c_{14})

2.2. Nanofluids processing

"As-received" nanoclays were used in the preparation of the nanofluids, according to a two-step protocol as reported by Maheswaran and Sunil (2016). A fixed concentration of 2 wt.% nanoclay was chosen for this preliminary study. First, the corresponding quantity of nanoclay was pre-dispersed in 25 g approx. castor oil in small glass vessels by using a small magnetic stirrer, at 50 ºC and for 45 minutes. Subsequently, the samples were sonicated in a Power Sonic 405 sonication bath at its maximum power, also at 50 ºC and for 45 minutes. In all cases, visual inspection allowed concluding that the dispersion quality was good.

Storage stability was used as a first criterion to carry out a screening on the potential use of the nanofluids. Thus, these were stirred and subsequently poured into test tubes and let evolve for 24 hours. The storage stability was qualitatively assessed by visual inspection of the interface between the settling dispersion and the sediment, according to Kang et al. (2019). The most stable nanofluids passed onto the subsequent electro-rheological (ER) and electro-tribological (ET) characterization. Only selected unstable nanofluids were also studied for the sake of comparison.

2.3. Nanofluids characterization

Steady viscous flow curves at 25 ºC were performed at increasing values of the DC electric field up to 4 kV/mm, in a shear rate interval from 0.1 to 100 s^{-1}. The strain-controlled ARES G2 rheometer (TA Instruments), equipped with a special electro-rheocell, a Keysight 33210A (Agilent) electric field generator and a Trek 609E-6 high-voltage power amplifier, was used. A plate-plate geometry with 25 mm diameter and 0.5 mm measuring gap was selected. In such a way, it was possible to evaluate the electro-rheological performance of the nanofluids based on the yield stress values arisen, at the lowest shear rates imposed, under the action of electric potentials. It was also possible to measure the current intensities through the fluid and so to calculate the corresponding leak current densities.

The polarizability of the nanoclays in castor oil was assessed by Broadband Dielectric Spectroscopy (BDS) measurements carried out with a Novocontrol Broadband Dielectric Spectrometer (Alpha-A High Performance Frequency Analyzer), at 1 V, in an AC frequency window between 1 Hz and 200 kHz. The liquid was confined in a special cell consisting of two brass electrodes with a 0.5 mm thick Teflon spacer in between. These tests allowed having a further insight into the electro-rheological potential of the fluids on a fast-track basis.

Moreover, an electro-tribocell consisting of a stainless steel ball (1.4401 grade 100) with 6.35 mm radius resting on three 45º pitched stainless steel plates (1.4301 AISI 304), coupled to the previously described ARES-G2 rheometer enabled to explore the friction performance under controlled electric fields. The friction coefficient was determined by applying transient tests (5 minutes of duration) at a fixed force of 5 N perpendicular to the plates' surface, and measuring the friction force at a sliding velocity of 22.45 mm/s (mixed lubrication regime), at increasing voltages up to 50 V.

All these tests were carried out, at least, three times for every sample.

3. Results and discussion

3.1. Study on the storage stability of the nanoclay dispersions

The nanofluids' storage stability was examined in order to discard unstable nanoclay/castor oil dispersions from further electro-rheological and electro-tribological analysis, thus reducing the number of samples to be studied. As previously explained, samples at 2 wt.% nanoclay were poured into test tubes and let evolve for 24 hours. Visual inspection allowed perceiving the effective dispersion of the freshly prepared fluids (t=0 h, in Figure 1). For the sake of a fast preliminary screening, the stability was qualitatively assessed by simple analysis of the solid settled at the tubes bottom. Figure 1a reveals that, in general, the organo-modified montmorillonites present quite good stability in castor oil after 24 h. Among them, those including dimethyl dihydrogenated-tallow quaternary ammonium, i.e. Cloisite 15A (15A), Cloisite 20A (20A) and Nanofil 15 (N15) or dimethyl benzyl hydrogenated-tallow quaternary ammonium, i.e. Nanofil SE3010 (SE3010), are more stable than that containing methyl tallow bis-2-hydroxyethyl quaternary ammonium, i.e. Cloisite 30B (30B), for which a slightly darker color can be observed at the tube bottom after 24 h. At first instance, the type of alkyl chains present in the organo-cation used in the first group of nanoclays seem to be contributing to a better stabilization of the platelets as compared to Cloisite 30B. A larger interlayer d_{001} distance (Table 1), due to more voluminous alkyl chains, in the first group of nanoclays may have enabled the oil molecules to enter the galleries more easily, thus improving their dispersion (Di Maio et al., 2015).

Regarding the natural nanoclays, a big contrast in terms of stability was observed between the phyllosilicates and the sepiolites. The halloysite nanotubes (Hal), the natural montmorillonite Closite Na^+ (C-Na^+) and the bentonites Volcanplus (VPlus) and Voncangel (Vgel) dispersions underwent severe phase separation after 24 h (Figure 1b), whilst the sepiolites Pansil, Pangel B20 (B20) and Pangel S9 (S9) showed very good stability (Figure 1c). In this case, the different stability is due to the effect of a much lower apparent density of the needle-like sepiolites (in fact, even much lower than the dispersing medium) as compared to the layered nanosilicates or nanotubes.

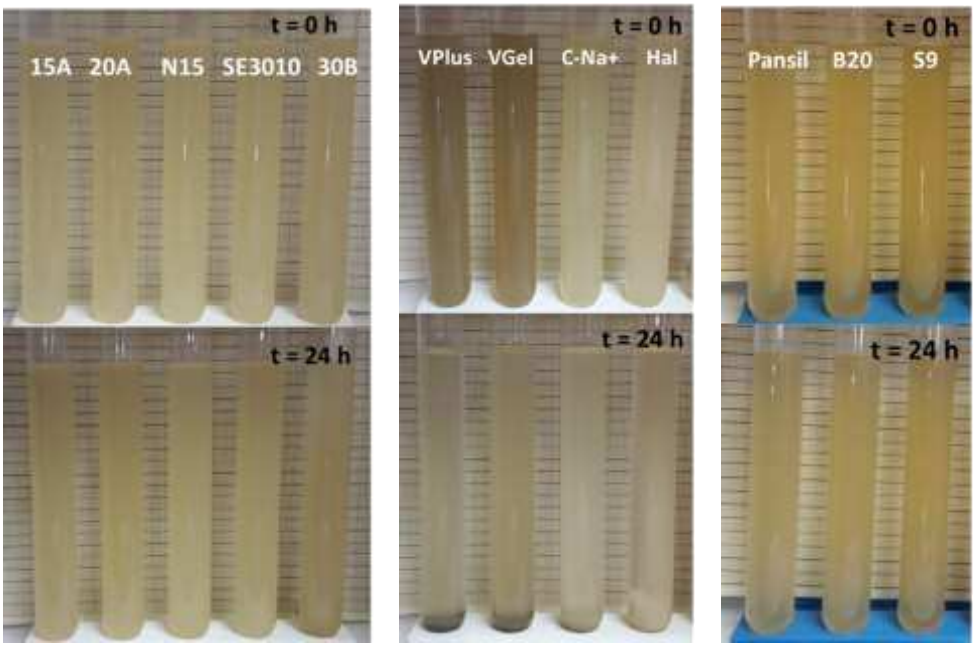

a) b) c)

Figure 1. Preliminary storage stability tests (freshly prepared dispersions and after 24 hours) for a) OMMT nanoclays, b) natural layered nanoclays and c) sepiolites.

3.2. Electro-rheological flow behavior of the nanoclay dispersions.

Only those nanofluids showing the best storage stability were electro-rheologically characterized. The electro-rheological potential was studied by means of flow curves in steady state at 25 ºC. Selected nanoclay dispersions are presented in Figures 2 and 3. As

225 deduced from the figures, these electro-rheological fluids correspond to the so-called
226 “Bingham” or “plastic” fluids, and their flow behavior was characterized by an electric
227 field dependent yield stress value at the lowest shear rates, followed by a Newtonian
228 evolution of the shear stress (τ) with the shear rate ($\dot{\gamma}$), according to Equation (1):

229 $$\tau(\dot{\gamma}, E) = \tau_y(E) + \eta_\infty \cdot \dot{\gamma} \qquad (1)$$

230 where $\tau_y(E)$ is the dynamic yield stress, η_∞ is the high-shear limiting Newtonian viscosity,
231 and E is the strength of the electric field applied (Chotpattananont et al., 2004). The off-
232 field test, included for reference, reveals the Newtonian behavior of the dispersions in the
233 absence of electric potential, i.e. a straight line with a slope of 1 in a double-log plot of
234 shear stress versus shear rate. The application of an electric potential originates a yield
235 stress that has to be overcome before the material starts flowing. The yield stress magnitude
236 increases with the electric field strength. There exists a balance between the electric force,
237 which arranges the polarized nanoclay particles into aligned structures, and the shear force,
238 which destroys them. Thus, the higher the field intensity, the higher the critical shear rate
239 at which the material behavior becomes Newtonian. Figure 2 shows flow curves, at 25 ºC,
240 at increasing electric fields up to 4 kV/mm for 2 wt.% dispersions of Cloisite 15A (a) and
241 Cloisite 30B (b), two representatives of the OMMT nanoclays studied. Despite their
242 different organo-cation and different storage stability (Figure 1a), they both showed very
243 high electro-rheological performance. At 4 kV/mm, their dynamic yield stress values were
244 of about 100 Pa. Moreover, at 1.60 kV/mm and higher intensities, their critical shear rates
245 values for the transition to the Newtonian behavior was beyond the upper limit of shear
246 rates studied, 100 s^{-1}.

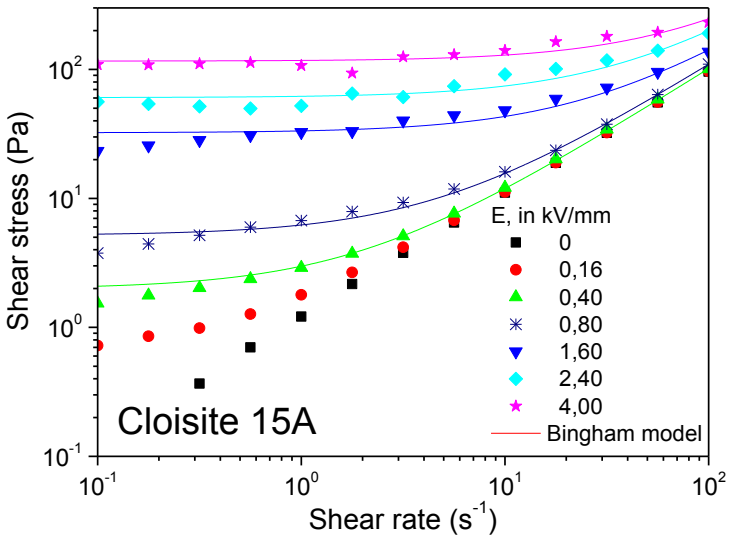

a)

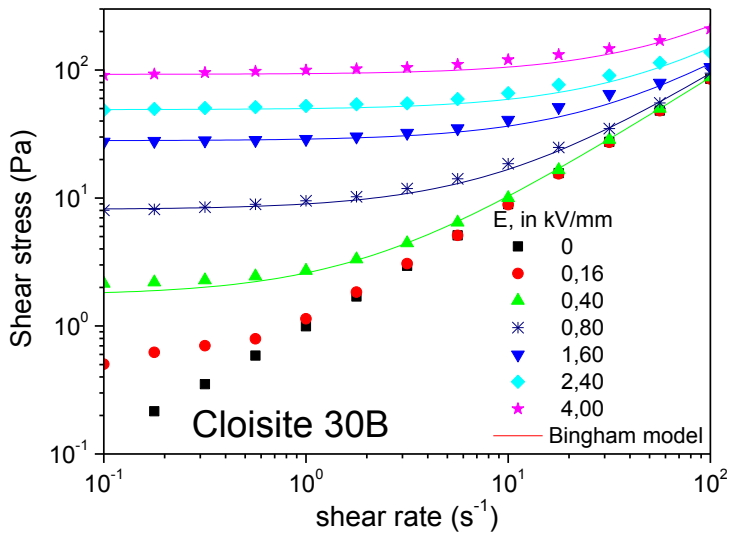

b)

Figure 2. Steady state flow curves at 25 ºC for 2 wt.% dispersions of a) Cloisite 15A and b) Cloisite 30B nanoclays in castor oil, as a function of electric field intensity.

The fiber-like sepiolite dispersions were also very stable after 24 hours of storage. An example of this type of clay is depicted in Figure 3a for the case of a 2 wt.% Pansil dispersion. Its rheological response in the absence of electric field was higher than that for the OMMT nanoclays studied, and slightly deviates from the Newtonian behavior. This is a typical viscous flow behavior that characterizes fiber/needle-like nanoclays due to their

capacity to form percolated networks, as reported in Kuznetsov et al. (2018a). Even so, it approached a limiting yield stress value of about 20 Pa with increasing the electric field intensity up to 4 kV/mm. So, the ER performance of this nanoclay was lower as compared to the OMMT nanoclays studied.

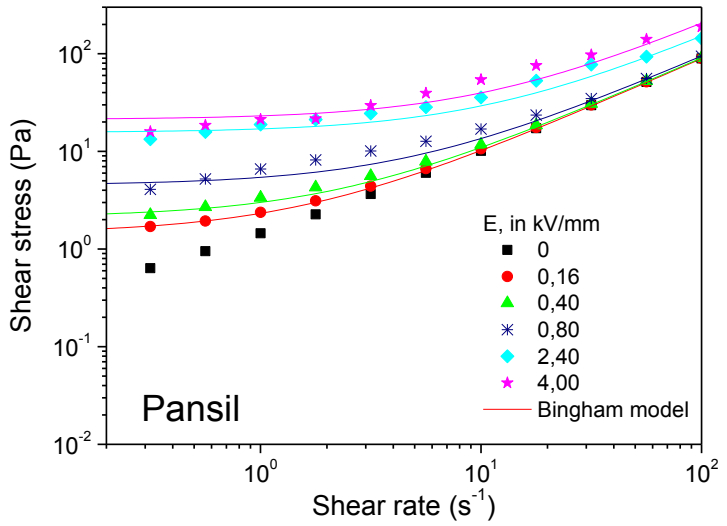

a)

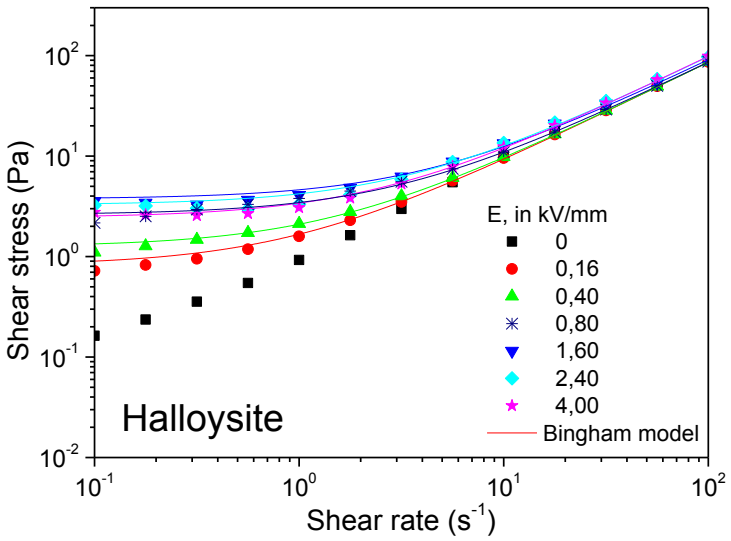

b)

Figure 3. Steady state flow curves at 25 ºC for 2 wt.% dispersions of a) Pansil and b) halloysite nanoclays in castor oil, as a function of electric field intensity.

The halloysite nanotubes did not yield a stable dispersion. Even so, its ER behavior is shown in Figure 3b for the sake of comparison. The yield stress values observed were even lower than in the sepiolites, at comparable concentrations and electric field intensities. A maximum yield stress value of 4 Pa at 1.6 kV/mm was found, after which the yield stress slightly decreased. Moreover, even at the highest electric field intensities was the Newtonian behavior clearly achieved at the upper decade of shear rates tested.

Rozynek et al. (2013) reported a kaolinite (layered silicate) dispersion to have an improved ER response relative to a halloysite dispersion. The observed behavior was attributed to the way in which the two types of clays form structures during the "chain/column" formation. By using the WAXS technique on clay-paraffin wax blends that were previously suggested to an electric field, these authors demonstrated that the layered silicate particles preferentially arranged with their basal planes being parallel to the electric field direction, thus presenting a strong anisotropy. On the contrary, Halloysite/paraffin wax blends did not show any anisotropy at all, probably because their different and irregular shapes did not enable ordered structures. Moreover, microscopy observations allowed Ramos-Tejada et al. (2018) to conclude that the sepiolite needles arrange into shorter and weaker chains than the montmorillonites when subjected to an electric potential. Finally, Kuznetsov et al. (2018a) explained that interacting plates yield more strong chain-like structures than interacting tubes, due to a larger overlapping area in the former case. Based on the physical evidences provided by these previous studies, and aimed to help the readers to better interpret the ER results in Figures 2 and 3 above, we propose a schematic representation of the structures formed upon application of electric potentials in Figure 4.

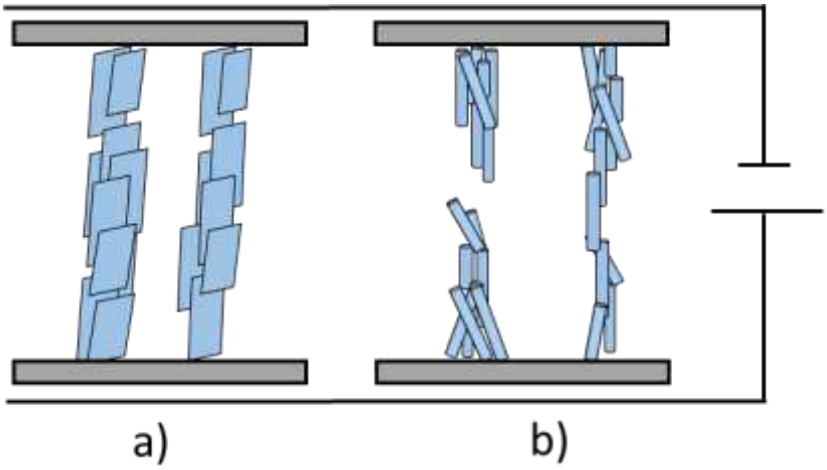

285 **Figure 4.** Schematic representation of the structures formed upon application of the electric field,
286 for: a) layered nanosilicates; b) tube-like/fiber-like nanoclays.

287 In terms of stability, it can be concluded that the Pansil dispersion in castor oil has proved
288 to be as good as the OMMT nanoclays dispersions. However, its ER potential is not too
289 high if compared to the above organo-modified layered nanosilicates. Thus, the OMMT
290 nanoclays seem to be a better candidate with a view to be used with electro-tribological
291 purpose.

292 The dynamic yield stress values, τ_y, as obtained from best fit of experimental data to
293 Equation (1), were plotted against the imposed electric field intensity in Figure 5. There
294 does not seem to be much difference between the different OMMT nanoclays studied, with
295 the exception of Nanofil SE3010, which demonstrated a lower ER capacity than the
296 remaining components of this group, although with a similar trend. For the OMMT
297 nanoclays, the evolution of τ_y with E, in the electric field range from 0.4 to 4 kV/mm, seems
298 to obey a power-law scaling, as expressed by Equation (2):

299 $$\tau_y(E) = a \cdot E^b \qquad (2)$$

300 In Equation (2), "a" corresponds, in fact, to the dynamic yield stress value at an electric
301 field intensity of 1 unit (in this case 1 kV/mm), and "b" is a parameter which according to

the classic polarization model, for an idealized ER fluid constituted by hard dielectric spheres treated as point dipole suspended in a Newtonian fluid, should have a value of 2. However, very often the value of "b" can deviate from the ideal value due to a list of possible causes which is a matter of debate (Liu and Choi, 2012; Seo et al., 2012). The "a" and "b" parameters, as obtained from best linear fit in double-log plots (Figure 5), are gathered in Table 2.

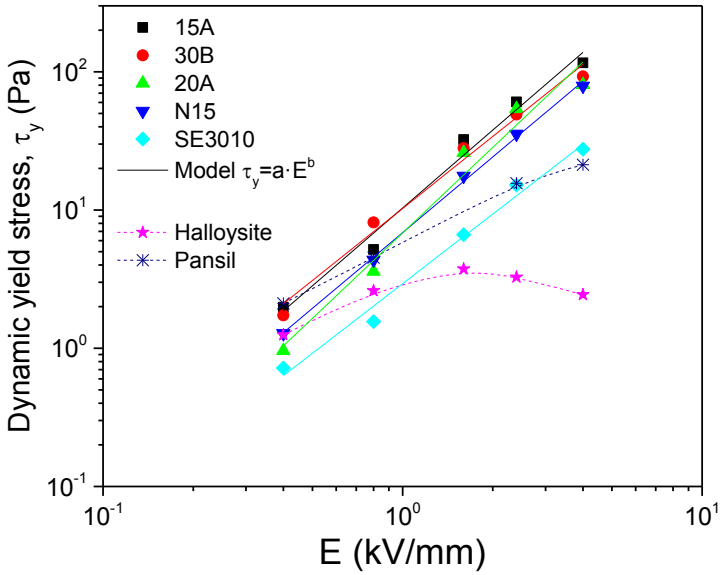

Figure 5. Evolution of the dynamic yield stress with the electric field intensity for selected 2 wt.% nanoclay dispersions in castor oil.

Regarding the halloysite and the Pansil nanoclays, they present a clear different behavior due to their lower ER potential. Their dynamic yield stress dependence with the electric field does not follow the Equation (2). The halloysite nanotubes show a maximum value of yield stress of 4 Pa at 1.60 kV/mm, after which the yield stress mildly decreases. Kuznetsov et al. (2018a) reported a similar evolution for concentrations of the "as received" halloysite of 1 and 2 wt.% in silicone oil, with the maximum value being shifted to higher E values. As for the Pansil fiber-like sepiolite, the evolution of the yield stress with E seems to approach asymptotically a limiting value. In both cases, it might be that if the particles

achieve their maximum polarization state, no further improvement in the chains structuring level is expected to occur. As later discussed, dielectric measurements may shed some light on this issue. Moreover, the halloysite nanoparticles, with different and irregular shapes, are known to randomly orientate and agglomerate when forming chains under the influence of electric fields (Rozynek et al., 2013). If the ER response is rather due to the formation of thick columns consisting of more or less random aggregates, the field-induced mechanical strength will be weakened (Ramos-Tejada et al., 2018). With time and stronger electric field strengths, a slight depletion may arise in this weak structure thus yielding some reduction in the yield stress.

Table 2. Fitting parameters of Equation (2) and measured values of $\Delta\varepsilon'$ and $\sigma_{AC,1Hz}$ for the different 2 wt.% OMMT nanoclays dispersions in castor oil.

Commercial Name	**"b" in Eq. (2)** [unitless]	**"a" in Eq. (2)** [Pa·(kV/mm)$^{-b}$]	**$\Delta\varepsilon'$** [unitless]	**$\sigma_{AC,1Hz}$** [S/cm]
Cloisite 15A	1.87	10.33	0.90	$5.0 \cdot 10^{-11}$
Cloisite 20A	2.01	6.82	0.70	$2.8 \cdot 10^{-11}$
Nanofil 15	1.82	6.86	0.59	$4.0 \cdot 10^{-11}$
Nanofil SE3010	1.67	2.93	0.51	$4.3 \cdot 10^{-11}$
Cloisite 30B	1.73	10.26	0.44	$8.9 \cdot 10^{-12}$

3.3. Dielectric characterization of the nanofluids

It is well known that the so-called "interfacial" or "Maxwell-Wagner" polarization is the main responsible for the electro-rheological mechanism (Lee et al., 2016). This type of polarization provoked by the electric field is due to the mismatch in dielectric constant between the particles and the dispersing medium (Chotpattananont et al., 2004). So, broadband dielectric spectroscopy (BDS) measurements were carried out on selected (optimal in terms of stability and ER potential) 2 wt.% nanoclay dispersions. The halloysite nanoclay did not yield a stable dispersion. Even so, it has been included for the sake of comparison, given its poor ER behavior. Moreover, the neat castor oil has also been

340 included as a reference. Figure 6 presents the evolution of the dielectric constant
341 (permittivity), ε', and dielectric loss, ε'', with AC frequency in the interval from 1 Hz to
342 200 kHz. The polarization rate is known to be one of the most important factors in
343 generating a high ER effect. It is quantified by the frequency at which the dielectric
344 relaxation (peak in the dielectric loss) occurs. According to Ikazaki et al. (1998) only
345 relaxation frequencies within 100 Hz and 100 kHz produce a significant ER effect.
346 Moreover, the dielectric relaxation produces a difference between the ε' values at both
347 sides of the frequency at which the relaxation peak appears, i.e. $\Delta\varepsilon' = \varepsilon_0' - \varepsilon_\infty'$. Thus, under
348 comparable relaxation frequencies, the higher the $\Delta\varepsilon'$, the stronger the ER effect will be
349 (Liu and Choi, 2012).

350 Regarding the OMMT nanoclays, Figure 6 demonstrates different behaviors because the
351 modifying agent introduced into the clay gallery alters its dielectric properties. It can be
352 observed a clear relaxation peak located at ca. 10 kHz for Cloisite 30B (containing methyl
353 tallow bis-2-hydroxyethyl quaternary ammonium ion), whilst the remaining modified
354 montmorillonites (including dimethyl dihydrogenated-tallow or dimethyl benzyl
355 hydrogenated-tallow quaternary ammonium ions) only exhibit a shoulder at ca. 5 kHz.

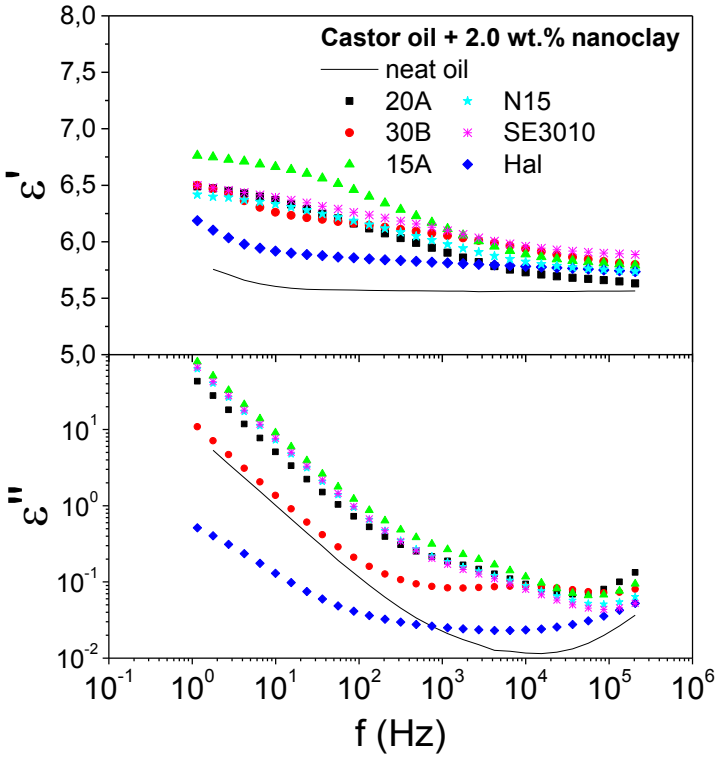

356 **Figure 6.** Evolution of dielectric constant and dielectric loss with frequency at 25 ºC for the
357 different 2 wt.% OMMT nanoclays dispersions (2 wt.% halloysite dispersion and neat castor oil
358 included for the sake of comparison).

359

360 Kuznetsov et al. (2018b) reported the use of a linear combination of the Havriliak–Negami
361 equation with conductivity to approximate experimental data of Cloisite 30B and Nanofil
362 SE3010 in polydimethylsiloxane. The model successfully described the dependence of the
363 dielectric loss on frequency as a result of the contribution of different relaxation
364 mechanisms associated to the "capacitors" formed by the various structures which may be
365 present in the dispersion (tactoids, intercalated and/or exfoliated particles). It is noteworthy
366 that only those structures which produce a relaxation within the measurable frequency
367 range are of interest. According to that model, and given the frequency values at which the
368 relaxation peaks in Figure 6 appear (5 to 10 kHz), these would be mainly a consequence of
369 what the authors referred to as "capacitors" of the first type (capacitors formed by the

presence of oil between tactoids in the dispersion) and the second type (capacitors due to the charges located between the platelets inside the stacks). However, the relaxation peak in Cloisite 30B is more notorious than in the remaining OMMT nanoclays. This result is a consequence of a relaxation peak which is not masked by the contribution of a high conductivity (Kuznetsov et al., 2018b), as occurs with the other OMMT nanoclays. In fact, lower ε´´ values at low frequencies denote lower conductivity. Moreover, Figure 7 probes the higher AC conductivity of Cloisite 15A, Nanofil 15, Nanofil SE3010 and Cloisite 20A as compared to Cloisite 30B. These fluids exhibited a low frequency AC conductivity plateau (i.e., in actuality the DC conductivity) that demonstrated their facility to form percolated conductive networks even at very low potentials (Roman et al., 2020). This represents an increase in AC conductivity, in some cases, of more than half decade as compared to Cloisite 30B and to castor oil. The σ_{AC} values at 25 ºC and 1 Hz are collected in Table 2.

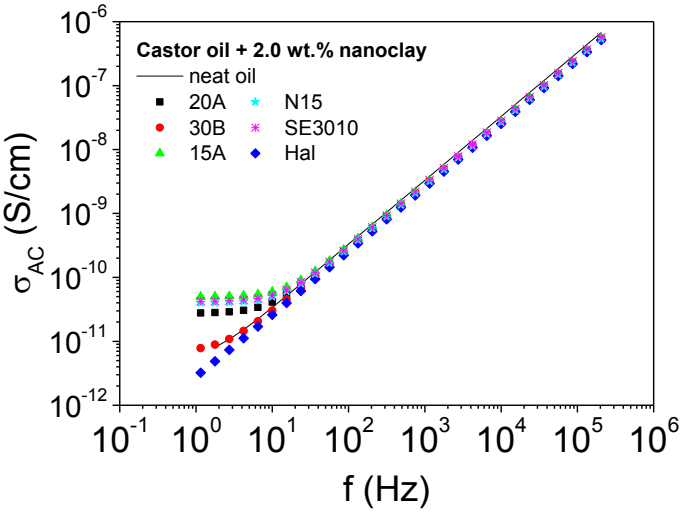

Figure 7. Evolution of AC conductivity with frequency at 25 ºC for the different 2 wt.% OMMT nanoclays dispersions (2 wt.% halloysite dispersion and neat castor oil included for the sake of comparison).

Furthermore, the magnitude of the polarization can be evaluated by comparing the measured values of $\Delta\varepsilon' = \varepsilon_0' - \varepsilon_\infty'$, with 10 Hz and 200 kHz being chosen as representative frequencies at the left (f_0) and right (f_∞) sides, respectively, of the relaxation peak. These values are shown in Table 2 for the whole set of OMMT nanoclays studied.

In some cases, a good linear correlation of the yield stress τ_y (and also the critical $\dot{\gamma}$ upon which the Newtonian behavior starts) with the particle polarizability, equally well represented by both the particle dipole coefficient, β, and the drop in permittivity, $\Delta\varepsilon'$, has been reported (Ikazaki et al., 1998; Lengalova et al., 2003). In that sense, the "a" parameter in Equation (2), i.e. the interpolated dynamic yield stress at 1 kV/mm from linear regression in double-log scale, was plotted versus the polarization capacity of the suspended particles, $\Delta\varepsilon'$, as illustrated in Figure 8. With the exception of the Cloisite 30B montmorillonite, which showed a higher performance than expected from its corresponding $\Delta\varepsilon'$ value, a fairly good linear dependency was found. The presence of two hydroxyethyl chains in the quaternary ammonium of Cloisite 30B, which are expected to promote some chemical affinity with the –OH groups located on the ricinoleic chains of the castor oil, might be affecting the measured value of $\Delta\varepsilon'$.

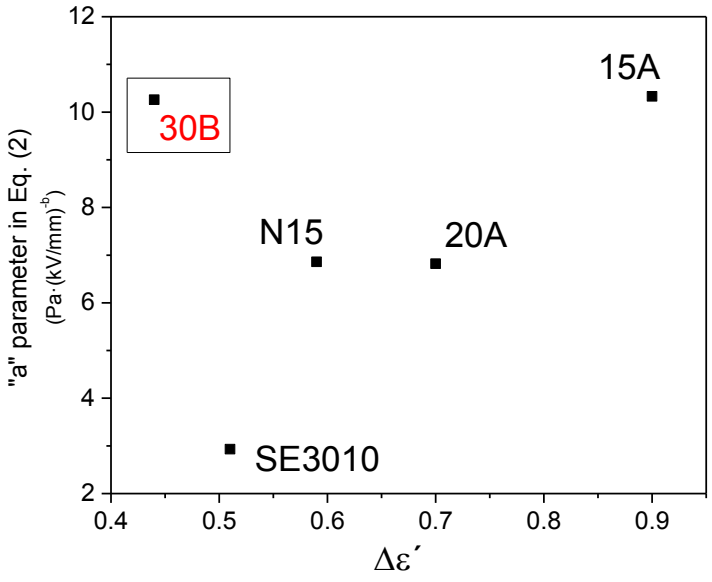

Figure 8. Relationship between the "a" parameter in Equation (2) and the permittivity drop $\Delta\varepsilon'$ for the different 2 wt.% OMMT nanoclays dispersions in castor oil.

Regarding the "b" parameter in Equation (2), all the values in Table 2 were comprised between the "theoretical" limits established by the polarization (b=2) and conduction (b=1.5) models (Zhang et al., 2020; Han et al., 2017). However, we were unable to establish any type of relationship since there must probably be several coupled factors affecting the results like conductivity, volume fraction, particle shape, or the way the particles interact to form chains (Chotpattananont et al., 2004; Ramos-Tejada et al., 2018).

For halloysite dispersions in polydimethylsiloxane, Kuznetsov et al. (2020) found a relaxation peak, which was attributed to a list of possible origins: charge transfer inside the tubes, particle interaction, and the formation of a percolation network at high concentrations. In our case, no transition in ε'' was detected for 2 wt.% halloysite dispersions in castor oil in the frequency range of interest (Figure 6). In fact, not even for a concentration as high as 6 wt.% halloysite was the relaxation in ε'' noticed (results not shown here). However, the evolution of ε' with frequency in Figure 6 matches that reported in Kuznetsov et al. (2020), with a not too noticeable drop in the permittivity, $\Delta\varepsilon'$. If the polarizability of this type of particle is small, the electrical torque tending to orientate them in the E-field direction will be also small, hence yielding a less organized chaining process. Regarding the AC conductivity of the 2 wt.% halloysite dispersion in castor oil in Figure 7, no evidence of electrical percolation (low frequency AC conductivity plateau) was observed, as also shown in Kuznetsov et al. (2020). In conclusion, the low value of $\sigma_{AC,1Hz}$ supports a low number of columnar structures formed under the action of an electric field. Furthermore, the low value of $\Delta\varepsilon'$ and the specific morphological characteristics of the filler (Kuznetsov et al., 2018a) bring about less organized structures. Hence, these must be

431 the reasons behind the poor ER performance of halloysite nanotubes observed in Figure 5,
432 as compared to the OMMT nanoclays.

433 It is worth noting the importance of the leakage current in practical applications of ER
434 fluids as smart materials. On the one hand, minimizing the unwanted large power
435 consumption is always a serious concern in an ER application. However, on the other hand,
436 too low conductivity values may be a sign of poor chain formation, thus poor ER effects.
437 Trying to shed some light on the issue, the electric field intensity dependence of the leak
438 current density, J(E), is presented in Figure 9 for selected samples. The group of clays
439 constituted by Cloisite 15A, Cloisite 20A, Nanofil 15 and Nanofilm SE3010, for which an
440 AC conductivity plateau was depicted in Figure 7, presents a fairly good linear dependency,
441 thus obeying the Ohm's law $V=I \cdot R$, in the E-field range considered. Even though the AC
442 conductivity value of Cloisite 30B was similar to that of the oil (Figure 7), the results in
443 Figure 9 support that, if subjected to large enough electric field intensities, this clay can
444 also arrange into structures which enable leak current. Thus, Cloisite 30B exhibits a power-
445 law relationship that can be represented by the general equation $J \propto E^n$ (Rozynek et al.,
446 2010). In any case, our OMMT nanoclays dispersions have demonstrated J(E) values which
447 do not entail large energy consumptions (Goswami et al., 2014). The halloysite nanotubes
448 presented a constant and extremely low value of J within the entire E-field range studied,
449 even slightly lower to that for neat castor oil, a result which corroborates the AC
450 conductivity behavior in Figure 7. A similar result was found for the Pansil needle-like
451 particles. Rozynek et al. (2010) reported that leak current density increases when chain
452 bridges spanning two electrodes are being formed. It might be that most of the chains are
453 not long enough so as to span the two measuring plates (Ramos-Tejada, 2018). In that
454 sense, both the upper and lower plates would be coated by a number of structures which

neither promote continuity (Figure 4b), thus yielding low conductivity, nor endow the fluid with a great ER effect.

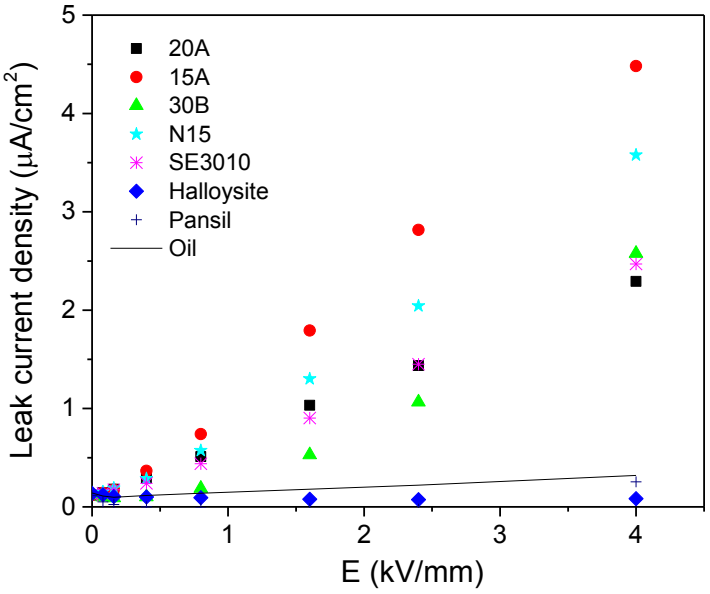

Figure 9. Electric field intensity dependence of the leak current density for selected 2 wt.% nanoclay dispersions in castor oil (neat castor oil included for the sake of comparison).

3.4. On the active control of the friction coefficient through electric potentials.

From the previous study, it seems fair to conclude on the higher potential of the OMMT nanoclays, relative to the other clays studied, so as to constitute the particulate phase of electro-sensitive lubricants based on castor oil. Moreover, among the whole set of OMMT nanoclays characterized, the Closite 15A nanoclay stands out because of its optimal balance of good storage stability, adequate dielectric properties and strong ER performance. For this reason, preliminary electro-tribological tests at 25 ºC were conducted on an optimal formulation prototype consisting in 2 wt.% Cloisite 15A dispersion in castor oil, up to 50 V, under 5 N load and 22.45 mm/s. This sliding velocity corresponds to a

lubrication region on which fluid friction and deformation of asperities (solid friction) are most probably involved.

In general, the entrance of nanoparticles into the contact point has been reported to have, to some extent, various possible effects: a) causing a protective effect by coating the rough friction surfaces, b) producing a polishing effect that reduces the roughness, or c) even compensating for the loss of mass, which is known as mending effect (Lee et al., 2009). More specifically, regarding the phyllosilicates, three possible mechanisms have been reported (Chizhik et al., 2019): i) due to their weakly bound layered structure, the platelets will easily shear and thus lubricate, once entering the contact; ii) the shearing process may release oxygen atoms that can passivate the metal surface, thereby reducing friction and wear; iii) adsorption at the surface that reduce the effective surface roughness. As for the nanotubes, the improvement in tribological properties has been related to exfoliation that yields a protecting tribofilm that effectively lowers metal-metal contact and provides a "rolling bearing" effect due to the tubular shape of the nanoparticles (Peña-Paras et al., 2017).

Figure 10 illustrates the evolution of the coefficient of friction (COF) with time, for a sequence of 5 consecutive steps (5 min. duration each) at increasing ΔV values from 0 up to 50 V. A reference curve at 0 V is also displayed for the sake of reference. The curve was obtained as the result of 5 consecutive steps set at 0 V, thereby yielding a final curve that is not continuous.

As expected, even in the absence of electric potential (reference curve, solid line), a time dependent decrease in the COF value was observed as a consequence of an initial roughness reduction due to the relative motion of the contact surfaces, until the final steady behavior was achieved. The application of a program with 5 increasing ΔV steps up to 50 V yielded a faster decay rate of the COF, over the 5 to 10 V steps, which resulted in an effective

reduction of ca. 9 %. Under the very small distances in the lubrication zone, even moderate electric potentials may produce an intense polarization effect on the nanoclay particles. In that sense, particle polarization and the effect of the electric potential may contribute to lure the particulate phase into the contact point, thus increasing and maintaining the concentration of layered nanosilicate particles (that migrate from the outer part of the bearing) at the location where they may effectively perform their lubrication role according to the mechanisms previously detailed (Chizhik et al., 2019). Moreover, exfoliated layers of the clay mineral will orientate under the electric field thus yielding the formation of structures that, consequently, may cause an important viscosity enhancement, as shown in Figure 2. Under the above lubrication regime, the two surfaces are not fully separated by the fluid film, thereby a higher-viscosity lubricant is expected to improve the friction behavior (Barber et al., 2005). Even so, further research is still needed before we can conclude on the specific origin of the observed behavior (purely electro-viscous/electro-physical, bulk/interfacial mechanisms, affected by other electro-chemical considerations) and whether these smart lubricants may also yield an improved wear behavior of the steel surfaces.

Kimura et al. (1994) reported a more substantial decrease in the COF when an electric field was applied across a liquid crystal film (biphenyls and esters) working in the boundary regime. A reduction in the COF of about 25 % was observed and attributed to ordered nematic phase structures in the liquid crystal upon application of 30 V. However, to the best of our knowledge, our present work is the first to report results on the active control of the tribological performance of the lubricant film under electric potentials using a 100 % environmentally friendly fluid (only made of castor oil and OMMT nanoclay).

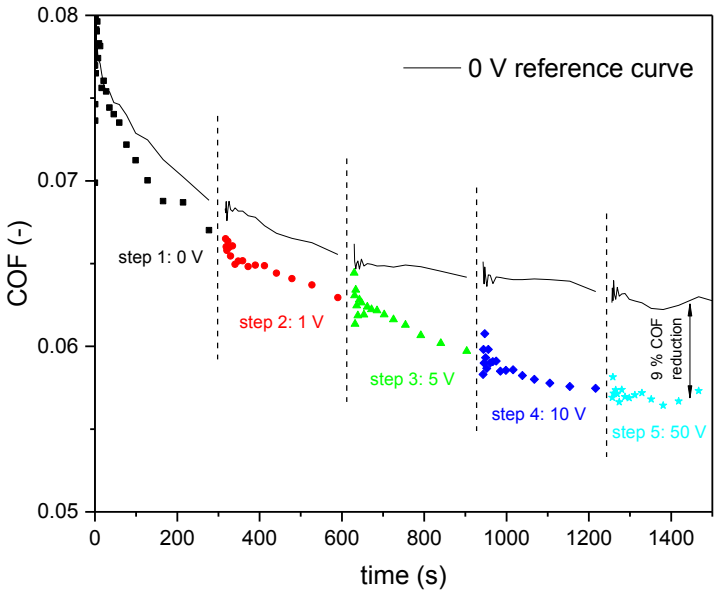

519 **Figure 10.** Evolution of the coefficient of friction with time in a sequence of 5 consecutive steps
520 with increasing electric potentials up to 50 V, using a 2 wt.% Closite 15A dispersion in castor oil
521 (test at 0 V included as reference).

522

523 # 4. Conclusions

524 Preliminary results on the development of 100 % ecofriendly electro-sensitive lubricating
525 fluids, based on nanoclay and castor oil, have been reported. In general, the organo-
526 modified montmorillonites and the sepiolites presented quite good stability in castor oil
527 after 24 h. Regarding the electro-rheological behavior, all the 2 wt.% dispersions studied
528 demonstrated Newtonian (or nearly) behavior in the absence of electric potential. Under
529 the action of electric fields their behavior turned into the so-called "Bingham" fluid. In
530 general, the OMMT nanoclays showed very high electro-rheological performance
531 (dynamic yield stress values in the vicinity of 100 Pa at 4 kV/mm). Inversely, the Pansil
532 sepiolite approached a limiting yield stress value of about 20 Pa with increasing the electric
533 field intensity up to 4 kV/mm, whilst the halloysite nanotubes exhibited a maximum yield
534 stress value of 4 Pa at 1.6 kV/mm. The observed behaviors were attributed to the formation
535 of stronger chain-like structures from interacted plates rather than tubes or fibers. As for

the dielectric properties, it was found a clear relaxation peak in ε´´ located at ca. 10 kHz for Cloisite 30B and a shoulder at ca. 5 kHz for the remaining OMMT nanoclays, in both cases related to interfacial polarization. For the OMMT nanoclays, in general, it was possible to correlate the dynamic yield stress values at 1 kV/mm with the drop in the permittivity, Δε´. With relation to the halloysite nanoclay, no transition in ε´´ was identified in the frequency range of interest. Finally, a reduction of the COF of ca. 9 % was obtained with the application of electric potentials up to 50 V using an optimal formulation prototype consisting in 2 wt.% Cloisite 15A dispersion in castor oil.

It seems fair to conclude that, in terms of storage stability, dielectric properties and ER/ET performance, our OMMT nanoclay dispersions in castor oil meet the requirements so as to be good candidates for a further and more comprehensive electro-tribological analysis. Further research is still needed before we can conclude on the specific origin of the observed behavior and whether these smart lubricants may also yield an improved wear behavior of the steel surfaces.

5. Declaration of Conflicting Interests

The authors declare no potential conflicts of interest with respect to the research, authorship, and/or publication of this article.

6. Acknowledgements

This work is part of a Research Project sponsored by "Programa Operativo FEDER-Andalucía 2014-2020" (UHU-1255843). The authors gratefully acknowledge its financial support. S.D. Fernández-Silva acknowledges the program "Ayudas para la promoción de empleo joven e implantación de la Garantía Juvenil en I+D+i en el Subprograma Estatal de Incorporación, del Programa Estatal de Promoción del Talento y su Empleabilidad en

559 I+D+i" (PEJ2018-003949-A) for funding his research contract. M. García-Morales and C.
560 Roman also acknowledge Vicerrectorado de Investigación y Transferencia (Universidad
561 de Huelva) for funding their research period at the Faculty of Electrical Engineering,
562 "Gheorghe Asachi" Technical University of Iasi (Romania).

563 7. References

564 Barber, G.C., Jiang, Q.Y., Zou, Q., Carlson, W., 2005. Development of a Laboratory Test
565 Device for Electrorheological Fluids in Hydrostatic Lubrication. Tribotest J. 11-3, 185-
566 191.

567 Chen, Z., Zhang, X., Xu, H.X., Li, J., Dong, J., 2011. Tribological Characteristics of
568 Combined Layered Phosphate and Silicate Additives in Mineral Oil. Tribol. Lett. 43, 197-
569 203.

570 Chizhik, P., Dietzel, D., Bill, S., Schirmeisen, A., 2019. Tribological properties of a
571 phyllosilicate based microparticle oil additive. Wear 426-427, 835-844.

572 Chotpattananont, D., Sirivat, A., Jamieson, A.M., 2004. Scaling of Yield Stress of
573 Polythiophene Suspensions under Electric Field. Macromol. Mater. Eng. 289, 434–441.

574 Di Maio, L., Garofalo, E., Scarfato, P., Incarnato, L., 2015. Effect of Polymer/Organoclay
575 Composition on Morphology and Rheological Properties of Polylactide Nanocomposites.
576 Polym. Compos. 36, 1135-1144.

577 Dold, C., Amann, T., Kailer, A., 2015. Influence of electric potentials on friction of sliding
578 contacts lubricated by an ionic liquid. Phys. Chem. Chem. Phys. 17, 10339-10342.

579 Garcia-Lopez, D., Fernandez, J.F., Merino, J.C., Santaren, J., Pastor, J.M., 2010. Effect of
580 organic modification of sepiolite for PA 6 polymer/organoclay nanocomposites. Compos.
581 Sci. Techn. 70, 1429–1436.

582 Gorbacheva, S.N., Yarmush, Y.M., Ilyin, S.O., 2020. Rheology and tribology of ester-
583 based greases with microcrystalline cellulose and organomodified montmorillonite. Tribol.
584 Int. 148, 106318 (13 pp).

585 Goswami, S., Brehm, T., Filonovich, S. Cidade, M.T., 2014. Electrorheological properties
586 of polyaniline-vanadium oxide nanostructures suspended in silicone oil. Smart Mater.
587 Struct. 23, 105012 (10 pp).

588 Han, W.J., Piao, S.H., Choi, H.J., 2017. Synthesis and electrorheological characteristics of
589 polyaniline@attapulgite nanoparticles via Pickering emulsion polymerization. Mater. Lett.
590 204, 42–44.

591 Ikazaki, F., Kawai, A., Uchida, K., Kawakami, T., Edamura, K., Sakuraik, K., Anzaik, H.,
592 Asako, Y., 1998. Mechanisms of electrorheology: the effect of the dielectric property. J
593 Phys. D: Appl. Phys. 31, 336-347.

Kang, X., Xia, Z., Chen, R., Sun, H., Yang, W., 2019. Effects of inorganic ions, organic polymers, and fly ashes on the sedimentation characteristics of kaolinite suspensions. App. Clay. Sci. 181, 105220 (12 pp).

Kimura, Y., Nakano, K., Kato, T., 1994. Wear 175, 143-149.

Kollias, A., Dimarogonas, A.D., 1994. Electro-rheological Fluid Flow in Partial Journal Bearings. In: ASME Winter Annual Meeting, Electro-Rheological Flows, Chicago.

Korenaga, A., Yoshioka, T., Mizutani, H., Kikuchi, K., 1999. Elastohydrodynamic Lubrication Characteristics of Electrorheological Fluids. In: Lubrication at the Frontier, Elsevier Science B.V., D. Dowson et al. (Editors), 517-522.

Kuznetsov, N.M., Shevchenko, V.G., Belousov, S.I., Chvalun, S.N., 2020. Dielectric Properties of Halloysite Nanotube Suspensions in Polydimethylsiloxane. Rus. J. Phys. Chem. A 94(2) 376–381.

Kuznetsov, N.M., Stolyarova, D.Y., Belousov, S.I., Kamyshinsky, R.A., Orekhov, A.S., Vasiliev, A.L., Chvalun, S.N., 2018a. Halloysite nanotubes: Prospects in electrorheology. Express Polym. Lett. 12(11), 958–965.

Kuznetsov, N.M., Shevchenko, V.G., Stolyarova, D.Y., Ozerin, S.A., Belousov, S.I., Chvalun, S.N., 2018b. Dielectric properties of modified montmorillonites suspensions in polydimethylsiloxane. J. Appl. Polym. Sci. 46614 (9 pp).

Lee, K., Hwang, Y., Cheong, S., Choi, Y., Kwon, L., Lee, J., Kim, S.H., 2009. Understanding the Role of Nanoparticles in Nano-oil Lubrication. Tribol. Lett. 35, 127–131.

Lee, S., Kim, Y.K., Hong, J-Y., Jang, J., 2016. Electro-response of MoS2 Nanosheets-Based Smart Fluid with Tailorable Electrical Conductivity. ACS Appl. Mater. Interfaces 8, 24221−24229.

Lengalova, A., Pavlikek, V., Saha, P., Stejskal, J., Kitano, T., Quadrat, O., 2003. The effect of dielectric properties on the electrorheology of suspensions of silica particles coated with polyaniline. Physica A 321, 411–424.

Liu, Y.D., Choi, H.J., 2012. Electrorheological fluids: smart soft matter and characteristics. Soft Matter 8, 11961-11978.

Madanhire, I., Mbohwa, C., 2016. Chapter 2: Lubricant Additive Impacts on Human Health and the Environment. In: Mitigating Environmental Impact of Petroleum Lubricants, Springer International Publishing, Switzerland.

Maheswaran, R., Sunil, J., 2016. Effect of nano sized garnet particles dispersion on the viscous behavior of extreme pressure lubricant oil. J. Mol. Liq. 223, 643-651.

Martín-Alfonso, J.E., Martín-Alfonso, M.J., Franco, J.M., 2020. Tunable rheological-tribological performance of “green” gel-like dispersions based on sepiolite and castor oil for lubricant applications. App. Clay Sci. 192, 105632 (9 pp).

Nikolakopoulos, P.G., Papadopoulos, C.A., 1996. High Speed Journal Bearings Lubricated with Electrorheological Fluids: an Experimental Investigation. Int. J. Modern Phys. B 10(23&24), 3045–3055.

Nikolakopoulos, P.G., Papadopoulos, C.A., 1998. Controllable High Speed Journal Bearings, Lubricated with Electrorheological Fluids: an Analytical and Experimental Approach. Trib. Int. 31(5), 225–234.

Peña-Parás, L., Maldonado-Cortés, D., García, P., Irigoyen, M., Taha-Tijerina, J., Guerra, J., 2017. Tribological performance of halloysite clay nanotubes as green lubricant additives. Wear 376-377, 885–892.

Peña-Parás, L., Maldonado-Cortés, D., Castillo, F., Leal, J., Garza, S., 2018. Application of nanoclay lubricants for lowering wear of tools for steel meshing - A case study. IOP Conf. Series: Mater. Sci. Eng. 400, 072004 (8 pp.).

Peña-Parás, L., Maldonado-Cortés, D., Rodríguez-Villalobos, M., Romero-Cantú, A.G., Montemayor, O.E., Herrera, M., Trousselle, G., González, J., Hugler, W., 2019. Optimization of milling parameters of 1018 steel and nanoparticle additive concentration in cutting fluids for enhancing multi-response characteristics. Wear 426-427, 877–886.

Peng, J., Zhu, K.Q., 2005. Hydrodynamic Characteristics of ER Journal Bearings with External Electric Field Imposed on the Contractive Part. J. Intell. Mater. Syst. Struct. 16, 493-499.

Polanský, R., Kadlec, P., Kolská, Z., Švorčík, V., 2017. Influence of dehydration on the dielectric and structural properties of organically modified montmorillonite and halloysite nanotubes. App. Clay Sci. 147, 19-27.

Quinchia, L.A., Delgado, M.A., Valencia, C., Franco, J.M., Gallegos, C., 2010. Viscosity modification of different vegetable oils with EVA copolymer for lubricant applications. Indust. Crops Prod. 32, 607–612.

Ramos-Tejada, M.M., Rodríguez, J.M., Delgado, A.V., 2018. Electrorheology of clay particle suspensions. Effects of shape and surface treatment. Rheol. Acta 57, 405-413.

Roman, C., Garcia-Morales, M., Goswami, S., Marques, A.C., Cidade, M.T., 2018. The electrorheological performance of polyaniline-based hybrid particles suspensions in silicone oil: influence of the dispersing medium viscosity. Smart Mater. Struct. 27, 075001 (13 pp).

Roman, C., Garcia-Morales, M., Olariu, M.A., McNally, T., 2020. Effect of selective distribution of MWCNTs on the solid-state rheological and dielectric properties of blends of PMMA and LDPE. J. Mater. Sci. 55, 8526-8540.

Rozynek, Z., Knudsen, K.D., Fossum, J.O., Meheust, Y., Wang, B., Zhou, M., 2010. Electric field induced structuring in clay–oil suspensions: new insights from WAXS, SEM, leak current, dielectric permittivity, and rheometry. J. Phys.: Condens. Matter 22, 324104 (8 pp).

Rozynek, Z., Zacher, T., Janek, M., Čaplovičová, M., Fossum, J.O., 2013. Electric-field-induced structuring and rheological properties of kaolinite and halloysite. App. Clay Sci. 77–78, 1–9.

Seo, Y.P., Choi, H.J., Seo, Y., 2011. Analysis of the flow behavior of electrorheological fluids with the aligned structure reformation. Polymer 52, 5695-5698.

Seo, Y.P., Choi, H.J., Seo, Y., 2012. A simplified model for analyzing the flow behavior of electrorheological fluids containing silica nanoparticle-decorated polyaniline nanofibers. Soft Matter 8, 4659-4663.

677 Taha-Tijerina, J., Aviña, K., Diabb, J.M., 2019. Tribological and Thermal Transport
678 Performance of SiO2-Based Natural Lubricants. Lubricants 7, 71 (11 pp.).

679 Wang, Z., Xia, Y., Liu, Z., 2011. Study the Sensitivity of Solid Lubricating Additives to
680 Attapulgite Clay Base Grease. Tribol. Lett. 42, 141-148.

681 Winslow, W.M., 1947. Method and means for translating electrical impulses into
682 mechanical force. U.S. Patent No. 2,417,850.

683 Yu, H.L., Wang, H.M., Yin, Y.L., Song, Z.Y., Zhou, X.Y., Ji, X.C., Wei, M., Shi, P.J., Bai,
684 Z.M., Zhang, W., 2021. Tribological behaviors of natural attapulgite nanofibers as an
685 additive for mineral oil investigated by orthogonal test method. Tribol. Int. 153, 106562
686 (11 pp.).

687 Zhang, K., Gao, C.Y., Choi, H.J., Yin, J., Zhao, X., 2020. Rheological analysis of titanium
688 dioxide nano-whisker based electrorheological fluids. J. Ind. Eng. Chem. 83, 285-288.